J. Appl. Comput. Mech., 5(1) (2019) 128-140
DOI: 10.22055/JACM.2018.25539.1277

ISSN: 2383-4536
jacm.scu.ac.ir

M&MoCS

Shahid Chamran
University of Ahvaz

Journal of
Applied and Computational Mechanics

Research Paper

# Buckling and Postbuckling of Concentrically Stiffened Piezo-Composite Plates on Elastic Foundations

**Mehdi Bohlooly[1], Keramat Malekzadeh Fard[2]**

[1] Aircraft Research Centre, Tehran, Iran

[2] Department of Structural Engineering and Simulation, Aerospace Research Institute
Malek Ashtar University of Technology, Tehran, Iran, kmalekzadeh@mut.ac.ir

Received April 16 2018; Revised June 08 2018; Accepted for publication June 10 2018.
Corresponding author: Keramat Malekzadeh Fard, kmalekzadeh@mut.ac.ir


**Abstract.** This research presents the modeling and analysis for the buckling and postbuckling behavior of sandwich plates under thermal and mechanical loads. The lay-up configurations of plates are laminated composite with concentric stiffener and surface mounted piezoelectric actuators. The plates are in contact with a three-parameter elastic foundation including softening and/or hardening nonlinearity. Several types of grid shapes of stiffeners are studied such as ortho grid, angle grid, iso grid, and orthotropic grid. The equations of structures are formulated based on the classical lamination theory incorporating nonlinear von-Karman relationships. The stress function and Galerkin procedure are applied to derive explicit formulations of the equilibrium paths. New results are introduced to give the influences of voltage through the thickness of piezoelectric actuators, different stiffeners, and nonlinear elastic foundations.

**Keywords**: Buckling; Composite; Stiffener; Piezoelectric; Foundation.

## 1. Introduction

The sandwich laminated composite plates and shells with concentric stiffeners are used in a huge number of aerospace structures due to their advantages such as low weight, high bending stiffness, low cost of manufacture, and most importantly, ability to carry considerable loads after buckling. Consequently, the researchers study on different grid shapes of stiffened structures to detect their effects on the stability of composite structures.

The classification of shapes and lay-up configurations of stiffened laminated composites are explained in detail by Li and Cheng [1] and Chen and Tsai [2]. In practical applications, four common grid shapes are used consist of ortho grid, angle grid, iso grid, and orthotropic grid. The presentation of a constitutive equation for above-mentioned grids is more important to achieve reliable formulations. Wodesenbet et al. [3] studied the mechanical buckling of iso grid stiffened composite cylinders. They used the smeared method to determine stiffness components of stiffened composite shells. In the smeared method, the force and moment resultants of stiffeners and laminates are calculated separately, and then, total resultants may be determined using the principle of superposition in terms of volume fractions. Moreover, free vibration of angle grid stiffened composite shells using the smeared method presented by Hemmatnezhad et al. [4] and [5]. However, , it is proved that the smeared method is not acceptable recently [6]. Other methods such as Lekhnitsky (Lekhnitskii) technique is suitable only for ortho grid shapes, which is used on the postbuckling and dynamic behavior of eccentrically stiffened FGM plates and shells [7, 8]. The general method of Lekhnitsky technique is presented by Chen and Tsai [2] for all grid shapes.

In the field of stability of stiffened composite plates, panels, and shells using experimental setup, Zhu et al. [9] presented the experimental study of the buckling and postbuckling of eccentrically stiffened aluminum panels with ortho grid shapes under the combined compression and shear loads. Moreover, Zhu et al. [10] tested the uniaxial compression of ortho grid stiffener with I-shape ribs in the postbuckling range. This type of stiffener with the laminated composite plate is tested by Wang et al. [11]. In other work, Villani et al. [12] tested adhesively bonded ortho grid stiffened homogenous panels under shear loads. Besides these works, some researchers studied the buckling and postbuckling behavior of stiffened composites using the finite element method. Huang et al. [13] using triangular curved shell element for laminates and curved beam element for ribs, studied the buckling analysis of four common types of grids in stiffened laminated composite plates. Zhao and Kapania [14] analyzed the buckling of new and innovative grid shapes using the finite element method and utilizing both shell and beam elements. Furthermore, the finite element analysis of ortho grid stiffeners with I-shape and T-shape ribs stiffened composite panels presented by Sudhirsastry et al. [15].

In the case of analytical methods, Wang and Abdalla [16] worked on the buckling of ortho grid, angle grid, and iso grid shapes of stiffened laminated composite plates and shells using the smeared method. Vescovini and Bisagni [17] using Ritz method presented the buckling of ortho grid stiffeners with omega-shape ribs stiffened plates. In the case of analytical methods, Nie et al. [18] presented an explicit solution for postbuckling of L-shape ortho grid stiffened composite plates. Nevertheless, the thermal and mechanical stability of stiffened laminated piezo-composite plates with different grid shapes have not been investigated.

In this study, an analytical approach of buckling and postbuckling of stiffened laminated composite plates with surface mounted piezoelectric actuators on nonlinear elastic foundations is presented. The derivations of equations are based on the classical lamination theory. The nonlinear equilibrium paths (closed form relations of load-maximum deflection) are derived by using the Galerkin procedure. In the numerical study, different comparisons confirm the accuracy of current results. Moreover, the effects of different grid shapes, piezoelectric actuators, and nonlinear elastic foundations on the buckling values and even postbuckling curves are investigated.

## 2. Governing Equations

Suppose a rectangular stiffened laminated piezo-composite plate having length $a$, width $b$, and total thickness $h$, which is resting on the nonlinear elastic foundation. The stiffened part of plate is reinforced by five various grid shapes such as ortho grid, angle grid, iso grid1, iso grid2, and orthotropic grid as a concentric stiffener in lay-up configuration which is shown in Fig. 1. In geometrical parameters of stiffener, $d_{11s}$, $d_{22s}$ and $d_{12s}$ denote the width of transversal, longitudinal, and diagonal ribs, respectively. In addition, $S_{11s}$, $S_{22s}$ and $S_{12s}$ are the distance between two parallel transversal, longitudinal, and diagonal ribs, respectively. The thicknesses of stiffened part, laminated composite, and actuators are defined by $h_s$, $2h_c$ and $h_a$, respectively. The angle of diagonal ribs ($\theta$) is referenced from $x$ coordinate.

According to the classical laminated plate theory [19, 20], the displacement fields $(u, v, w)$ are introduced in terms of displacement components of the middle surface $(u_0, v_0, w_0)$ as follows:

$$
\begin{aligned}
u(x,y,z) &= u_0(x,y) - z\frac{\partial}{\partial x}w_0(x,y) \\
v(x,y,z) &= v_0(x,y) - z\frac{\partial}{\partial y}w_0(x,y) \\
w(x,y,z) &= w_0(x,y)
\end{aligned}
\tag{1}
$$

The relationships between small strains $(\varepsilon_{xx}, \varepsilon_{yy}, \gamma_{xy})$ and moderately large displacements based on von-Karman assumption are [20, 21]:

$$
\begin{aligned}
\varepsilon_{xx} &= \frac{\partial}{\partial x}u + \frac{1}{2}(\frac{\partial}{\partial x}w)^2 \\
\varepsilon_{yy} &= \frac{\partial}{\partial y}v + \frac{1}{2}(\frac{\partial}{\partial y}w)^2 \\
\gamma_{xy} &= \frac{\partial}{\partial y}u + \frac{\partial}{\partial x}v + \frac{\partial}{\partial x}w \times \frac{\partial}{\partial y}w
\end{aligned}
\tag{2}
$$

Equations (1) and (2) can be rewritten as:

$$
\begin{Bmatrix} \varepsilon_{xx} \\ \varepsilon_{yy} \\ \gamma_{xy} \end{Bmatrix} = \begin{Bmatrix} \varepsilon_{xx}^{(0)} + z\varepsilon_{xx}^{(1)} \\ \varepsilon_{yy}^{(0)} + z\varepsilon_{yy}^{(1)} \\ \gamma_{xy}^{(0)} + z\gamma_{xy}^{(1)} \end{Bmatrix}
\tag{3}
$$

wherein:

$$\begin{Bmatrix} \varepsilon_{xx}^{(0)} \\ \varepsilon_{yy}^{(0)} \\ \gamma_{xy}^{(0)} \end{Bmatrix} = \begin{Bmatrix} \frac{\partial}{\partial x}u_0 + \frac{1}{2}(\frac{\partial}{\partial x}w_0)^2 \\ \frac{\partial}{\partial y}v_0 + \frac{1}{2}(\frac{\partial}{\partial y}w_0)^2 \\ \frac{\partial}{\partial y}u_0 + \frac{\partial}{\partial x}v_0 + \frac{\partial}{\partial x}w_0 \times \frac{\partial}{\partial y}w_0 \end{Bmatrix}, \quad \begin{Bmatrix} \varepsilon_{xx}^{(1)} \\ \varepsilon_{yy}^{(1)} \\ \gamma_{xy}^{(1)} \end{Bmatrix} = -\begin{Bmatrix} \frac{\partial^2}{\partial x^2}w_{0,xx} \\ \frac{\partial^2}{\partial y^2}w_0 \\ 2\frac{\partial^2}{\partial x \partial y}w_{0,xy} \end{Bmatrix} \tag{4}$$

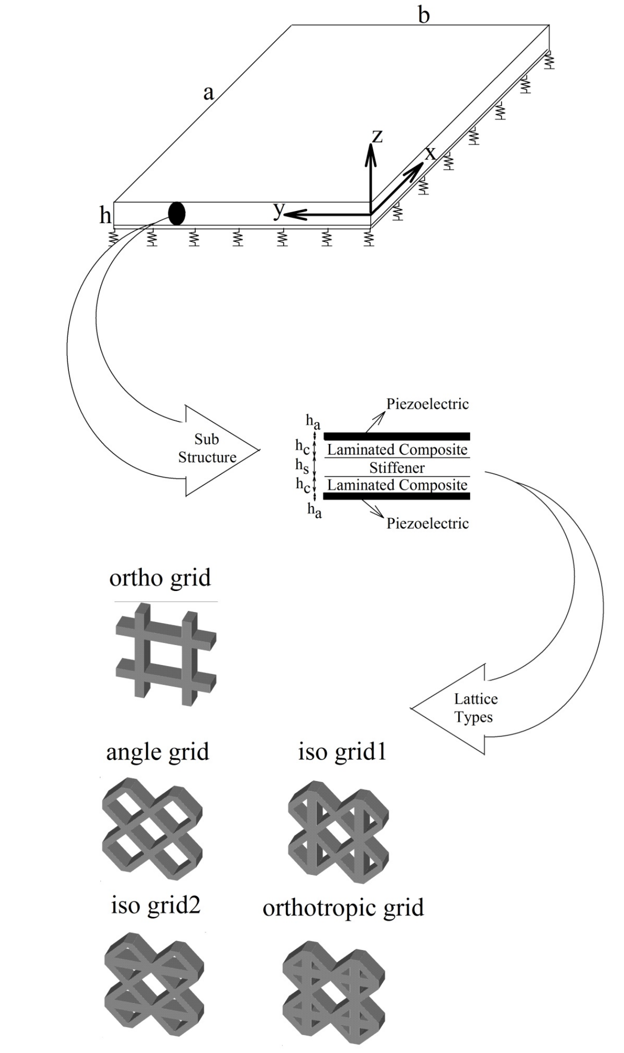


**Fig. 1.** A stiffened piezoelectric-composite plate on elastic foundation.

In this investigation, the laminated composite is made of $N$ perfect laminas in which all orthotropic laminas have same thickness. In each lamina, unidirectional fibers are embedded in a polymer base matrix. The constitutive equation of an arbitrary $k^{th}$ lamina with angle $(\alpha)$ corresponding to the $x$ axis is defined as:

$$\begin{pmatrix} \sigma_{xx} \\ \sigma_{yy} \\ \tau_{xy} \end{pmatrix}_k = \begin{pmatrix} \bar{Q}_{11} & \bar{Q}_{12} & \bar{Q}_{16} \\ \bar{Q}_{21} & \bar{Q}_{22} & \bar{Q}_{26} \\ \bar{Q}_{16} & \bar{Q}_{26} & \bar{Q}_{66} \end{pmatrix}_k \begin{pmatrix} \varepsilon_{xx} - \alpha_x \Theta \\ \varepsilon_{yy} - \alpha_y \Theta \\ \gamma_{xy} - \alpha_{xy} \Theta \end{pmatrix}_k \tag{5}$$

where the detailed description of Eq. (5) may be found in [22, 23]. Hooke's law for different shapes of stiffeners is defined as:

$$\begin{pmatrix} \sigma_{xx} \\ \sigma_{yy} \\ \sigma_{ss} \end{pmatrix} = \begin{pmatrix} Q_{11}^s & Q_{12}^s & Q_{16}^s \\ Q_{12}^s & Q_{22}^s & Q_{26}^s \\ Q_{16}^s & Q_{26}^s & Q_{66}^s \end{pmatrix} \begin{pmatrix} \varepsilon_{xx} \\ \varepsilon_{yy} \\ \gamma_{ss} \end{pmatrix} \tag{6}$$

where

$$\begin{pmatrix} Q_{11}^s & Q_{12}^s & Q_{16}^s \\ Q_{12}^s & Q_{22}^s & Q_{26}^s \\ Q_{16}^s & Q_{26}^s & Q_{66}^s \end{pmatrix} = \begin{pmatrix} \rho\dfrac{d_{11s}E_{stiff}}{S_{11s}} + \lambda\dfrac{2d_{12s}E_{stiff}}{S_{12s}}c^4 & \lambda\dfrac{2d_{12s}E_{stiff}}{S_{12s}}c^2s^2 & 0 \\ \lambda\dfrac{2d_{12s}E_{stiff}}{S_{12s}}c^2s^2 & \psi\dfrac{d_{22s}E_{stiff}}{S_{22s}} + \lambda\dfrac{2d_{12s}E_{stiff}}{S_{12s}}s^4 & 0 \\ 0 & 0 & \lambda\dfrac{2d_{12s}E_{stiff}}{S_{12s}}c^2s^2 \end{pmatrix} \tag{7}$$

Here, $c$ and $s$ denote sine and cosine of $\theta$, respectively and ( $\rho, \psi, \lambda$ ) are defined according to five various grid shapes as:

$$\begin{array}{lll} \text{angle grid:}(0,0,1) & \text{iso grid1:}(0,1,1) & \text{iso grid2:}(1,0,1) \\ \text{ortho grid:}(1,1,0) & \text{orthotropic grid:}(1,1,1) & \end{array} \tag{8}$$

The stress components of piezoelectric material in the shape of thin plate may be written as [24, 25]:

$$\begin{pmatrix} \sigma_{xx} \\ \sigma_{yy} \\ \tau_{xy} \end{pmatrix} = \begin{pmatrix} Q_{11}^a & Q_{12}^a & 0 \\ Q_{21}^a & Q_{22}^a & 0 \\ 0 & 0 & Q_{66}^a \end{pmatrix} \begin{pmatrix} \varepsilon_{xx} - \alpha_x^a\Theta \\ \varepsilon_{yy} - \alpha_y^a\Theta \\ \gamma_{xy} - \alpha_{xy}^a\Theta \end{pmatrix} - \begin{pmatrix} 0 & 0 & e_{31} \\ 0 & 0 & e_{32} \\ 0 & 0 & 0 \end{pmatrix} \begin{pmatrix} E_x \\ E_y \\ E_z \end{pmatrix} \tag{9}$$

where the in-plane electric field components $(E_x, E_y)$ have null values. The transverse component can be written as [20, 25] $E_z = V_a / h_a$. The resultant form of constitutive relations can be calculated as [26]:

$$\begin{aligned} &\begin{Bmatrix} N_x \\ N_y \\ N_{xy} \end{Bmatrix} + \begin{Bmatrix} N_x^T \\ N_y^T \\ N_{xy}^T \end{Bmatrix} + \begin{Bmatrix} N_x^E \\ N_y^E \\ N_{xy}^E \end{Bmatrix} = \left\{ \begin{pmatrix} Q_{11}^s & Q_{12}^s & Q_{16}^s \\ Q_{12}^s & Q_{22}^s & Q_{26}^s \\ Q_{16}^s & Q_{26}^s & Q_{66}^s \end{pmatrix} I_1^s + \begin{Bmatrix} Q_{11}^a & Q_{12}^a & 0 \\ Q_{12}^a & Q_{22}^a & 0 \\ 0 & 0 & Q_{66}^a \end{Bmatrix} I_1^a \right. \\ &\left. + \begin{pmatrix} A_{11} & A_{12} & A_{16} \\ A_{12} & A_{22} & A_{26} \\ A_{16} & A_{26} & A_{66} \end{pmatrix} \right\} \begin{Bmatrix} \varepsilon_{xx}^{(0)} \\ \varepsilon_{yy}^{(0)} \\ \gamma_{xy}^{(0)} \end{Bmatrix} + \begin{pmatrix} B_{11} & B_{12} & B_{16} \\ B_{12} & B_{22} & B_{26} \\ B_{16} & B_{26} & B_{66} \end{pmatrix} \begin{Bmatrix} \varepsilon_{xx}^{(1)} \\ \varepsilon_{yy}^{(1)} \\ \gamma_{xy}^{(1)} \end{Bmatrix} \end{aligned} \tag{10a}$$

$$\begin{aligned} &\begin{Bmatrix} M_x \\ M_y \\ M_{xy} \end{Bmatrix} + \begin{Bmatrix} M_x^T \\ M_y^T \\ M_{xy}^T \end{Bmatrix} = \begin{pmatrix} B_{11} & B_{12} & B_{16} \\ B_{12} & B_{22} & B_{26} \\ B_{16} & B_{26} & B_{66} \end{pmatrix} \begin{Bmatrix} \varepsilon_{xx}^{(0)} \\ \varepsilon_{yy}^{(0)} \\ \gamma_{xy}^{(0)} \end{Bmatrix} + \left\{ \begin{pmatrix} Q_{11}^s & Q_{12}^s & Q_{16}^s \\ Q_{12}^s & Q_{22}^s & Q_{26}^s \\ Q_{16}^s & Q_{26}^s & Q_{66}^s \end{pmatrix} I_3^s \right. \\ &\left. + \begin{Bmatrix} Q_{11}^a & Q_{12}^a & 0 \\ Q_{12}^a & Q_{22}^a & 0 \\ 0 & 0 & Q_{66}^a \end{Bmatrix} I_3^a + \begin{pmatrix} D_{11} & D_{12} & D_{16} \\ D_{12} & D_{22} & D_{26} \\ D_{16} & D_{26} & D_{66} \end{pmatrix} \right\} \begin{Bmatrix} \varepsilon_{xx}^{(1)} \\ \varepsilon_{yy}^{(1)} \\ \gamma_{xy}^{(1)} \end{Bmatrix} \end{aligned} \tag{10b}$$

where $I_i^s$, $I_i^a$, extensional stiffness $(A_{ij})$, coupling stiffness $(B_{ij})$, bending stiffness $(D_{ij})$, and the resultants of electrical and thermal loads are given in appendix A.

## 3. Equilibrium Equations

The nonlinear equilibrium equations of a rectangular stiffened piezolaminated composite plate may be derived according to the variational principle [24, 27]. Since the external loads $P_x$ and $P_y$ are present, the total potential energy of the structure is equal to the potential energy of external loads beside the strain energy of structure and foundation. Therefore, in a statically equilibrium position one can express:

$$\begin{aligned} V &= \frac{1}{2}\iiint \left[ \sigma_{xx}\left(\varepsilon_{xx} - \alpha_x\Theta\right) + \sigma_{yy}\left(\varepsilon_{yy} - \alpha_y\Theta\right) + \tau_{xy}\left(\gamma_{xy} - \alpha_{xy}\Theta\right) - E_z D_z \right] dxdydz \\ &+ \frac{1}{2}\iint \left\{ k_0 w^2 + k_1[(\frac{\partial}{\partial x}w)^2 + (\frac{\partial}{\partial y}w)^2] + \frac{1}{2}k_2 w^4 \right\} dxdy \\ &+ \iint \left[ \frac{P_x}{b}(\frac{\partial}{\partial x}u) + \frac{P_y}{a}(\frac{\partial}{\partial y}v) \right] dxdy \end{aligned} \tag{11}$$

Here, the foundation interactions are modeled by parameters such as Winkler $(k_0)$, Pasternak $(k_1)$ and softening/hardening $(k_2)$ and the definition of electrical displacement $D_z$ may be found in [28]. Substituting Eqs. (3), (5), and (6) into Eq. (11) and integrating through thickness and then applying the variational principle to minimize the function of total potential energy result three equilibrium equations of plate as:

$$\begin{aligned}
&\frac{\partial}{\partial x}N_x + \frac{\partial}{\partial y}N_{xy} = 0 \\
&\frac{\partial}{\partial x}N_{xy} + \frac{\partial}{\partial y}N_y = 0 \\
&N_x \frac{\partial^2}{\partial x^2}w_0 + 2N_{xy}\frac{\partial^2}{\partial x \partial y}w_0 + N_y \frac{\partial^2}{\partial y^2}w_0 - k_0 w_0 - k_2 w_0^3 + k_1 \frac{\partial^2}{\partial x^2}w_0 \\
&+k_1 \frac{\partial^2}{\partial y^2}w_0 + \frac{\partial^2}{\partial x^2}M_x + 2\frac{\partial^2}{\partial x \partial y}M_{xy} + \frac{\partial^2}{\partial y^2}M_y = 0
\end{aligned} \tag{12}$$

In order to derive a unified equilibrium equation from above-mentioned equations, the stress function is defined as $N_x = \frac{\partial^2}{\partial y^2}\Phi,\ N_y = \frac{\partial^2}{\partial x^2}\Phi,\ N_{xy} = -\frac{\partial^2}{\partial x \partial y}\Phi$ . In Eq. (12), the first two equations are satisfied and final equilibrium equation is:

$$\begin{aligned}
&\Phi_{,yy}w_{0,xx} - 2\Phi_{,xy}w_{0,xy} + \Phi_{,xx}w_{0,yy} - k_0 w_0 - k_2 w_0^3 + k_1 w_{0,xx} + k_1 w_{0,yy} \\
&+\frac{\partial^2}{\partial x^2}M_x + 2\frac{\partial^2}{\partial x \partial y}M_{xy} + \frac{\partial^2}{\partial y^2}M_y = 0
\end{aligned} \tag{13}$$

Substituting Eq. (10.b) into Eq. (13) gives:

$$\begin{aligned}
&\Phi_{,yy}w_{0,xx} - 2\Phi_{,xy}w_{0,xy} + \Phi_{,xx}w_{0,yy} - k_0 w_0 - k_2 w_0^3 + k_1 w_{0,xx} + k_1 w_{0,yy} + \Phi_{,xxxx}\{AQ_{12}B_{11} + AQ_{22}B_{12}\} \\
&+\Phi_{,yyyy}\{AQ_{11}B_{12} + AQ_{12}B_{22}\} + \Phi_{,xxyy}\{AQ_{11}B_{11} + AQ_{22}B_{22} + 2AQ_{12}B_{12} - 2AQ_{66}B_{66}\} \\
&+w_{0,xxxx}\{AQ_{11}B_{11}^2 + 2AQ_{12}B_{12}B_{11} + AQ_{22}B_{12}^2 - (Q_{11}{}^s I_3{}^s + Q_{11}{}^a I_3{}^a + D_{11})\} \\
&+w_{0,yyyy}\{AQ_{11}B_{12}^2 + 2AQ_{12}B_{22}B_{12} + AQ_{22}B_{22}^2 - (Q_{22}{}^s I_3{}^s + Q_{22}{}^a I_3{}^a + D_{22})\} \\
&+w_{0,xxyy}\{2AQ_{11}B_{12}B_{11} + 2AQ_{12}B_{22}B_{11} + 2AQ_{12}B_{12}^2 + 2AQ_{22}B_{22}B_{12} \\
&+4AQ_{66}B_{66}^2 - 2(Q_{12}{}^s I_3{}^s + Q_{12}{}^a I_3{}^a + D_{12}) - 4(Q_{66}{}^s I_3{}^s + Q_{66}{}^a I_3{}^a + D_{66})\} = 0
\end{aligned} \tag{14}$$

The components of matrix $AQ$ is defined by:

$$AQ = \begin{pmatrix} Q_{11}{}^s I_1{}^s + Q_{11}{}^a I_1{}^a + A_{11} & Q_{12}{}^s I_1{}^s + Q_{12}{}^a I_1{}^a + A_{12} & Q_{16}{}^s I_1{}^s + Q_{16}{}^a I_1{}^a + A_{16} \\ Q_{12}{}^s I_1{}^s + Q_{12}{}^a I_1{}^a + A_{12} & Q_{22}{}^s I_1{}^s + Q_{22}{}^a I_1{}^a + A_{22} & Q_{26}{}^s I_1{}^s + Q_{26}{}^a I_1{}^a + A_{26} \\ Q_{16}{}^s I_1{}^s + Q_{16}{}^a I_1{}^a + A_{16} & Q_{26}{}^s I_1{}^s + Q_{26}{}^a I_1{}^a + A_{26} & Q_{66}{}^s I_1{}^s + Q_{66}{}^a I_1{}^a + A_{66} \end{pmatrix}^{-1} \tag{15}$$

## 4. Compatibility Equation

When the relationship between strain and displacement is linear, the corresponding compatibility equation is [22]:

$$\varepsilon_{xx,yy} + \varepsilon_{yy,xx} - \gamma_{xy,xy} = 0 \tag{16}$$

But for the nonlinearity of Eq. (2), it should be nonzero. On the other hand, substituting Eqs. (3) and (4) into the left side of Eq. (16) gives:

$$\varepsilon_{xx,yy} + \varepsilon_{yy,xx} - \gamma_{xy,xy} = w_{0,xy}{}^2 - w_{0,xx}w_{0,yy} \tag{17}$$

Applying Eq. (10.a) and stress functions gives the strains of middle surface as follows:

$$\begin{aligned}
&\varepsilon_{xx}{}^{(0)} = AQ_{11}[\Phi_{,yy} + N_x{}^T - \varepsilon_{xx}{}^{(1)}B_{11} - \varepsilon_{yy}{}^{(1)}B_{12}] + AQ_{12}[\Phi_{,xx} + N_y{}^T - \varepsilon_{xx}{}^{(1)}B_{12} - \varepsilon_{yy}{}^{(1)}B_{22}] \\
&\varepsilon_{yy}{}^{(0)} = AQ_{12}[\Phi_{,yy} + N_x{}^T - \varepsilon_{xx}{}^{(1)}B_{11} - \varepsilon_{yy}{}^{(1)}B_{12}] + AQ_{22}[\Phi_{,xx} + N_y{}^T - \varepsilon_{xx}{}^{(1)}B_{12} - \varepsilon_{yy}{}^{(1)}B_{22}] \\
&\gamma_{xy}{}^{(0)} = +AQ_{66}[-\Phi_{,xy} + N_{xy}{}^T - \gamma_{xy}{}^{(1)}B_{66}]
\end{aligned} \tag{18}$$

Again, substituting Eq. (18) into the left side of Eq. (16) and applying Eq. (3) gives:

$$\varepsilon_{xx,yy}+\varepsilon_{yy,xx}-\gamma_{xy,xy}=\begin{Bmatrix}+AQ_{11}[\Phi_{,yyyy}+w_{0,xxyy}B_{11}+w_{0,yyyy}B_{12}]\\+AQ_{12}[\Phi_{,xxyy}+w_{0,xxyy}B_{12}+w_{0,yyyy}B_{22}]\end{Bmatrix}$$
$$+\begin{Bmatrix}+AQ_{12}[\Phi_{,xxyy}+w_{0,xxxx}B_{11}+w_{0,xxyy}B_{12}]\\+AQ_{22}[\Phi_{,xxxx}+w_{0,xxxx}B_{12}+w_{0,xxyy}B_{22}]\end{Bmatrix}-\left\{AQ_{66}[-\Phi_{,xxyy}+2w_{0,xxyy}B_{66}]\right\} \tag{19}$$

Equations (17) and (19) are equal. Therefore, by simplifying two last equations, the compatibility equation of plate in terms of two unknowns $\Phi$ and $w_0$ may be obtained as:

$$AQ_{22}\Phi_{,xxxx}+AQ_{11}\Phi_{,yyyy}+(2AQ_{12}+AQ_{66})\Phi_{,xxyy}+[AQ_{12}B_{11}+AQ_{22}B_{12}]w_{0,xxxx}+[AQ_{11}B_{12}+AQ_{12}B_{22}]w_{0,yyyy}$$
$$+[AQ_{11}B_{11}+AQ_{22}B_{22}+2AQ_{12}B_{12}-2AQ_{66}B_{66}]w_{0,xxyy}=+w_{0,xy}{}^{2}-w_{0,xx}w_{0,yy} \tag{20}$$

## 5. Solving Equations

All four edges of the rectangular plate are supposed to be in simply supported conditions. However, two different cases of simply supported conditions are investigated. In the case of the plate under uniaxial or biaxial compression, the edges are freely movable [29]:

$$\begin{aligned}x=0,a:&\quad w=M_x=N_{xy}=0\\ y=0,b:&\quad w=M_y=N_{xy}=0\end{aligned} \tag{21a}$$

and in the case of the plate under thermal environment, the edges are fully immovable [30]:

$$\begin{aligned}x=0,a:&\quad u=w=M_x=0\\ y=0,b:&\quad v=w=M_y=0\end{aligned} \tag{21b}$$

According to above-mentioned conditions, the deflection and stress functions are approximated as follows:

$$w_0=W\sin\bar{m}x\sin\bar{n}y \tag{22a}$$

$$\Phi=C_1\cos 2\bar{m}x+C_2\cos 2\bar{n}y+C_3\cos 2\bar{m}x\cos 2\bar{n}y+C_4\sin\bar{m}x\sin\bar{n}y+\frac{1}{2}N_{x0}y^2+\frac{1}{2}N_{y0}x^2 \tag{22b}$$

where $\bar{m}=m\pi/a,\bar{n}=n\pi/b$ and also pre-buckling forces $N_{x0},N_{y0}$ are in the corresponding directions $x, y$. The unknown coefficients of stress function $C_i(i=1,2,3,4)$ can be obtained by the substitution of Eqs. (22.a) and (22.b) into Eq. (20):

$$C_1=\frac{W^2\bar{m}^2\bar{n}^2}{32\beta_1\bar{m}^4},\ C_2=\frac{W^2\bar{m}^2\bar{n}^2}{32\beta_2\bar{n}^4},\ C_3=0,\ C_4=-W\frac{\beta_6\bar{m}^2\bar{n}^2+\beta_5\bar{n}^4+\beta_4\bar{m}^4}{\beta_1\bar{m}^4+\beta_2\bar{n}^4+\beta_3\bar{m}^2\bar{n}^2} \tag{23}$$

wherein:

$$\begin{aligned}&\beta_1=AQ_{22}\ ,\beta_2=AQ_{11},\ \ \beta_3=2AQ_{12}+AQ_{66},\ \ \beta_4=AQ_{12}B_{11}+AQ_{22}B_{12},\\&\beta_5=AQ_{11}B_{12}+AQ_{12}B_{22},\ \ \beta_6=AQ_{11}B_{11}+AQ_{22}B_{22}+2AQ_{12}B_{12}-2AQ_{66}B_{66}\end{aligned} \tag{24}$$

The residue of the Galerkin method may be revealed with the substitution of Eqs. (22.a) and (22.b) into Eq. (14). To calculate the nonlinear algebraic equation of $W$, the residue should set orthogonal with respect to $\sin\bar{m}x\sin\bar{n}y$.

$$\begin{aligned}&-2WC_2\bar{m}^2\bar{n}^2+WC_4\bar{m}_o\bar{n}_o(\frac{96}{9ab})-W\bar{m}^2N_{x0}-2WC_1\bar{m}^2\bar{n}^2-W\bar{n}^2N_{y0}-Wk_0\\&-W^3k_2(\frac{9}{16})-Wk_1\bar{m}^2-Wk_1\bar{n}^2+16C_1\bar{m}^4\{AQ_{12}B_{11}+AQ_{22}B_{12}\}(-\frac{16}{3\bar{m}_o\bar{n}_oab})\\&+C_4\bar{m}^4\{AQ_{12}B_{11}+AQ_{22}B_{12}\}+16C_2\bar{n}^4\{AQ_{11}B_{12}+AQ_{12}B_{22}\}(-\frac{16}{3\bar{m}_o\bar{n}_oab})\\&+C_4\bar{n}^4\{AQ_{11}B_{12}+AQ_{12}B_{22}\}+C_4\bar{m}^2\bar{n}^2\{AQ_{11}B_{11}+AQ_{22}B_{22}+2AQ_{12}B_{12}-2AQ_{66}B_{66}\}\\&+W\bar{m}^4\{AQ_{11}B_{11}{}^2+2AQ_{12}B_{12}B_{11}+AQ_{22}B_{12}{}^2-(Q_{11}{}^sI_3{}^s+Q_{11}{}^aI_3{}^a+D_{11})\}\\&+W\bar{n}^4\{AQ_{11}B_{12}{}^2+2AQ_{12}B_{22}B_{12}+AQ_{22}B_{22}{}^2-(Q_{22}{}^sI_3{}^s+Q_{22}{}^aI_3{}^a+D_{22})\}\\&+W\bar{m}^2\bar{n}^2\{2AQ_{11}B_{12}B_{11}+2AQ_{12}B_{22}B_{11}+2AQ_{12}B_{12}{}^2+2AQ_{22}B_{22}B_{12}+4AQ_{66}B_{66}{}^2\\&-2(Q_{12}{}^sI_3{}^s+Q_{12}{}^aI_3{}^a+D_{12})-4(Q_{66}{}^sI_3{}^s+Q_{66}{}^aI_3{}^a+D_{66})\}=0\end{aligned} \tag{25}$$

in the above-mentioned equation, when $m$ and/or $n$ are even numbers, the terms which consist of $\overline{m}_o$ and $\overline{n}_o$ should be zero. Otherwise, $\overline{m}_o$, $\overline{n}_o$ are equal to $\overline{m}$, $\overline{n}$ .

### 5.1. Mechanical Loads

Suppose a stiffened laminated piezo-composite plate resting on a nonlinear elastic foundation under uniform in-plane compressions $P_x$ and $P_y$. Due to movable simply supported boundary conditions, the plate may buckle. In order to estimate the buckling and postbuckling behavior of the plate, the prebuckling forces are as:

$$\begin{pmatrix} N_{x0} \\ N_{y0} \\ N_{xy0} \end{pmatrix} = -\begin{pmatrix} P_x / b \\ RP_x / b \\ 0 \end{pmatrix}, \quad R = \frac{P_y / a}{P_x / b} \tag{26}$$

The explicit form of load-deflection relationship can be obtained by applying Eq. (26) into Eq. (25) as follows:

$$\begin{aligned} P_x / b = & \frac{W^2}{\overline{m}^2 + \overline{n}^2 R} \times \{ \frac{\beta_1 \overline{m}^4 + \beta_2 \overline{n}^4}{16\beta_1\beta_2} + \frac{9k_2}{16} \} + \frac{W}{\overline{m}^2 + \overline{n}^2 R} \frac{8\overline{m}_o\overline{n}_o}{3ab} \\ & \times \{ 4\frac{\beta_6 \overline{m}^2\overline{n}^2 + \beta_5 \overline{n}^4 + \beta_4 \overline{m}^4}{\beta_1 \overline{m}^4 + \beta_2 \overline{n}^4 + \beta_3 \overline{m}^2 \overline{n}^2} + \frac{\beta_4}{\beta_1} + \frac{\beta_5}{\beta_2} \} + \frac{1}{\overline{m}^2 + \overline{n}^2 R} \times \{ k_0 + k_1(\overline{m}^2 + \overline{n}^2) \\ & + \frac{(\beta_6 \overline{m}^2\overline{n}^2 + \beta_5 \overline{n}^4 + \beta_4 \overline{m}^4)^2}{\beta_1 \overline{m}^4 + \beta_2 \overline{n}^4 + \beta_3 \overline{m}^2 \overline{n}^2} - \overline{m}^4 B_{11}(AQ_{11}B_{11} + AQ_{12}B_{12}) - B_{12}(\overline{m}^4\beta_4 + \overline{n}^4\beta_5) \\ & - \overline{n}^4 B_{22}(AQ_{12}B_{12} + AQ_{22}B_{22}) - 4\overline{m}^2\overline{n}^2 AQ_{66}B_{66}{}^2 - 2\overline{m}^2\overline{n}^2 B_{12}(AQ_{11}B_{11} + AQ_{12}B_{12}) \\ & - 2\overline{m}^2\overline{n}^2 B_{22}\beta_4 + \overline{m}^4(Q_{11}{}^s I_3^s + Q_{11}{}^a I_3^a + D_{11}) + \overline{n}^4(Q_{22}{}^s I_3^s + Q_{22}{}^a I_3^a + D_{22}) \\ & + 2\overline{m}^2\overline{n}^2(Q_{12}{}^s I_3^s + Q_{12}{}^a I_3^a + D_{12}) + 4\overline{m}^2\overline{n}^2(Q_{66}{}^s I_3^s + Q_{66}{}^a I_3^a + D_{66}) \} \end{aligned} \tag{27}$$

The buckling load of the multi-material structure on the elastic foundation can be determined by condition $W = 0$ .

### 5.2. Thermal Loads

Assume a stiffened laminated piezo-composite plate on a nonlinear elastic foundation is subjected to a uniform temperature rise [31] $\Theta = \Delta T$ for all piezoelectric, composite, and stiffener parts. Due to immovable conditions, the plate would not be able to expand in length and width of the piezo-composite part. But transversal sides of ribs would have expansion in stiffener parts. Therefore, the thermal resultants in the piezo-composite part may be derived as:

$$\begin{Bmatrix} N_x{}^T \\ N_y{}^T \end{Bmatrix} = \Delta T \begin{Bmatrix} AQ_x{}^T \\ AQ_y{}^T \end{Bmatrix} \tag{28}$$

where $AQ_x{}^T$ and $AQ_y{}^T$ are listed in Appendix B. On the other hand, in the situation of immovable boundary conditions, the average end-shortening parameters [23, 29] are taken to be zero:

$$\int_0^b \int_0^a \frac{\partial u_0}{\partial x} dxdy = 0 \tag{29a}$$

$$\int_0^b \int_0^a \frac{\partial v_0}{\partial y} dxdy = 0 \tag{29b}$$

By applying Eqs. (4), (18), (22), and (28) in end-shortening integrals, the prebuckling forces may be derived as:

$$N_{x0} = \frac{1}{8} W^2 \frac{\overline{m}^2 AQ_{22} - \overline{n}^2 AQ_{12}}{AQ_{11}AQ_{22} - AQ_{12}{}^2} + C_4 \overline{n}^2 (\frac{4}{\overline{m}_o\overline{n}_o ab}) - \Delta T AQ_x{}^T + W\overline{m}^2 B_{11}(\frac{4}{\overline{m}_o\overline{n}_o ab}) + W\overline{n}^2 B_{12}(\frac{4}{\overline{m}_o\overline{n}_o ab}) \tag{30a}$$

$$N_{y0} = \frac{1}{8} W^2 \frac{\overline{m}^2 AQ_{12} - \overline{n}^2 AQ_{11}}{AQ_{12}{}^2 - AQ_{11}AQ_{22}} + C_4 \overline{m}^2 (\frac{4}{\overline{m}_o\overline{n}_o ab}) - \Delta T AQ_y{}^T + W\overline{m}^2 B_{12}(\frac{4}{\overline{m}_o\overline{n}_o ab}) + W\overline{n}^2 B_{22}(\frac{4}{\overline{m}_o\overline{n}_o ab}) \tag{30b}$$

Once again, when $m$ and or $n$ are even numbers, the terms which consist of $\overline{m}_o$ and $\overline{n}_o$ should be zero. Otherwise, $\overline{m}_o$, $\overline{n}_o$ are equal to $\overline{m}$, $\overline{n}$ . By substituting of Eqs. (30.a) and (30.b) in Eq. (25), the explicit form of temperature increment-deflection relationship can be obtained as follows:

$$\Delta T = \frac{W^2}{16(\bar{m}^2 AQ_x^T + \bar{n}^2 AQ_y^T)} \times \{2\frac{\bar{m}^4 AQ_{22} + \bar{n}^4 AQ_{11} - 2\bar{m}^2\bar{n}^2 AQ_{12}}{AQ_{11}AQ_{22} - AQ_{12}^2} + \frac{\beta_1\bar{m}^4 + \beta_2\bar{n}^4}{\beta_1\beta_2} + 9k_2\}$$
$$+\frac{W}{\bar{m}^2 AQ_x^T + \bar{n}^2 AQ_y^T} \times \frac{8\bar{m}_o\bar{n}_o}{3ab}\{\frac{\beta_6\bar{m}^2\bar{n}^2 + \beta_5\bar{n}^4 + \beta_4\bar{m}^4}{\beta_1\bar{m}^4 + \beta_2\bar{n}^4 + \beta_3\bar{m}^2\bar{n}^2} + \frac{3\bar{m}^2}{2\bar{n}^2}B_{11} + \frac{3\bar{n}^2}{2\bar{m}^2}B_{22} + 3B_{12} + \frac{\beta_4}{\beta_1} + \frac{\beta_5}{\beta_2}\}$$
$$+\frac{1}{\bar{m}^2 AQ_x^T + \bar{n}^2 AQ_y^T} \times \{-(\bar{n}^2 e_{32} 2V_a + \bar{m}^2 e_{31} 2V_a) + k_0 + k_1(\bar{m}^2 + \bar{n}^2) + \frac{(\beta_6\bar{m}^2\bar{n}^2 + \beta_5\bar{n}^4 + \beta_4\bar{m}^4)^2}{\beta_1\bar{m}^4 + \beta_2\bar{n}^4 + \beta_3\bar{m}^2\bar{n}^2} \quad (31)$$
$$-\bar{m}^4 B_{11}(AQ_{11}B_{11} + AQ_{12}B_{12}) - B_{12}(\bar{m}^4\beta_4 + \bar{n}^4\beta_5) - \bar{n}^4 B_{22}(AQ_{12}B_{12} + AQ_{22}B_{22}) - 4\bar{m}^2\bar{n}^2 AQ_{66}B_{66}^2$$
$$-2\bar{m}^2\bar{n}^2 B_{12}(AQ_{11}B_{11} + AQ_{12}B_{12}) - 2\bar{m}^2\bar{n}^2 B_{22}\beta_4 + \bar{m}^4(Q_{11}^s I_3^s + Q_{11}^a I_3^a + D_{11}) + \bar{n}^4(Q_{22}^s I_3^s + Q_{22}^a I_3^a + D_{22})$$
$$+2\bar{m}^2\bar{n}^2(Q_{12}^s I_3^s + Q_{12}^a I_3^a + D_{12}) + 4\bar{m}^2\bar{n}^2(Q_{66}^s I_3^s + Q_{66}^a I_3^a + D_{66})\}$$

Again, the temperature corresponding $W = 0$ means the critical buckling load of multi-structure on the elastic foundation.

## 6. Results and Discussions

Unlikely, there are not reliable references on the buckling and postbuckling of stiffened laminated composite plates with piezoelectric actuators. Therefore, the calculations of current investigation are validated by simplified conditions.

First, the mechanical buckling and postbuckling of simple isotropic plates under the uniaxial compression are compared with the study of Tung and Duc [31] in Fig. 2. The thickness of piezoelectric actuators and concentric stiffeners are taken to be zero and thickness of laminated composite $2h_c$ is 1. The material properties of composite are $E_{11} = E_{22} = 380\,GPa$, $\nu_{12} = 0.3$, $G_{12} = E_{11}/2(1+\nu_{12})$, $\alpha_{11} = \alpha_{22} = 7.4e-6\ 1/^oC$. In the next example, the previous plate under the thermal environment is compared with the other results of Tung and Duc [31] in Fig. 3. According to Figs. 2 and 3, the results of current calculations are well justified with those of Tung and Duc [31].

To demonstrate the use of postbuckling formulas for piezo-composite plates, a verification is carried out with the study of Shen [32] for loading conditions of thermal environment and voltages in Fig. 4. The lay-up configuration of plate is $[P/(0/90)_2]_S$ and the thermo-mechanical properties of composite laminas (Graphite-Epoxy) are $E_{11} = 150\,GPa$, $E_{22} = 9.0\,GPa$, $\nu_{12} = 0.3$, $G_{12} = 7.1\,GPa$, $\alpha_{11} = 1.1e-6\ 1/^oC$, $\alpha_{22} = 25.2e-6\ 1/^oC$ and the electro-thermo-mechanical properties for piezoelectric actuators (PZT-5A) are $E_{11} = 63\,GPa$, $E_{22} = 63\,GPa$, $\nu_{12} = 0.3$, $G_{12} = 24.2\,GPa$, $\alpha_{11} = 0.9e-6\ 1/^oC$, $\alpha_{22} = 0.9e-6\ 1/^oC$, $d_{11} = 2.54e-10\ m/V$, $d_{22} = 2.54e-10\ m/V$. The results of Shen [32] are obtained through the perturbation technique based on the higher order shear deformation theory of Reddy. As can be seen, that comparison is accurate and efficient for all voltages.

To assure the validity of the effect of nonlinear elastic foundation on the equilibrium paths, a verification is presented with the study of Zhang and Zhou [33] for the isotropic plate under the biaxial compressions. The three parameters of elastic foundation and loading are normalized as $K_0 = k_0 b^4/E_{22}h^3$, $K_1 = k_1 b^2/E_{22}h^3$, $K_2 = k_2 b^4/E_{22}h$, and $\lambda_x = P_x b/E_{22}h^3$. The material properties of composite are $E_{11} = E_{22} = 201.04\,GPa$, $\nu_{12} = 0.28, G_{12} = E_{11}/2(1+\nu_{12})$. The results of Zhang and Zhou [33] are derived by multi-term Ritz method based on the higher order shear deformation theory and an acceptable agreement can be observed in Fig. 5.

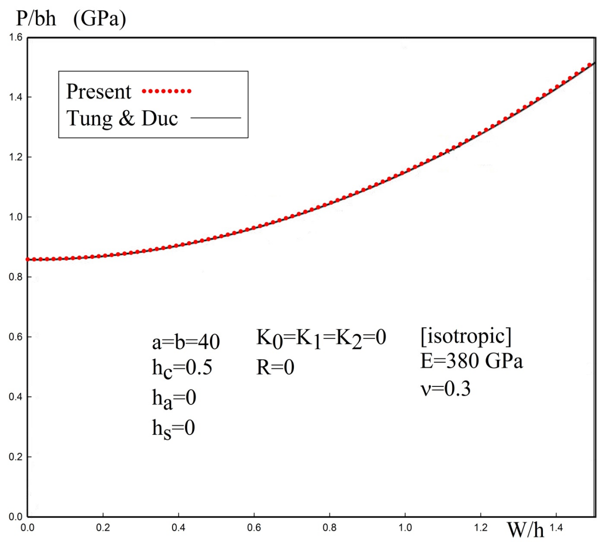


**Fig. 2.** Verifications of mechanical postbuckling.

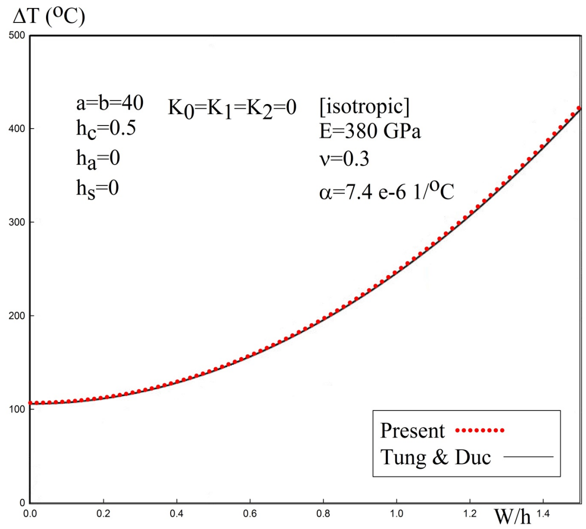


**Fig. 3.** Verifications of thermal postbuckling.

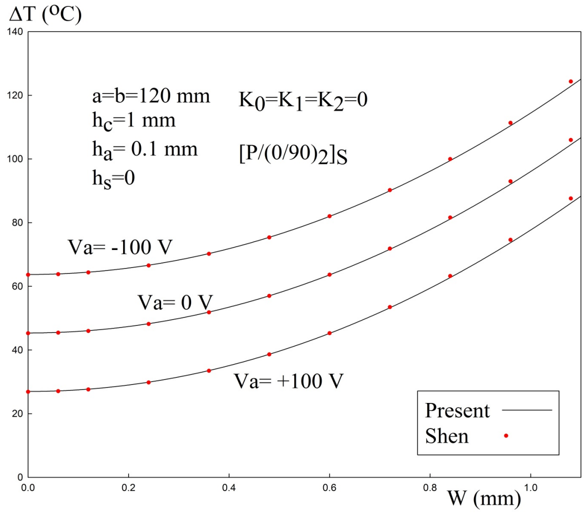


**Fig. 4.** Verifications of electro-thermal postbuckling.

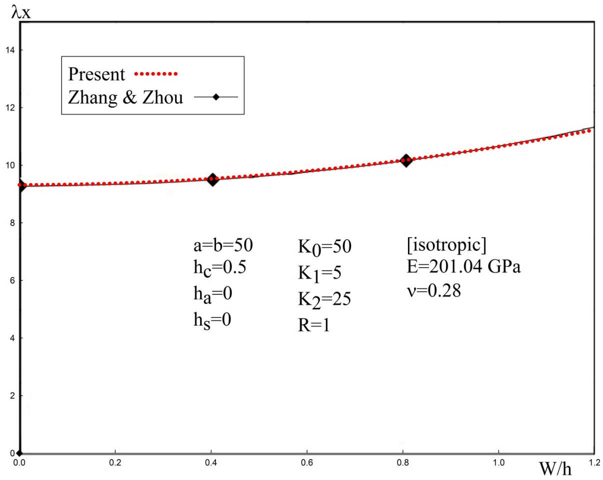


**Fig. 5.** Verifications of nonlinear elastic foundation on mechanical postbuckling.

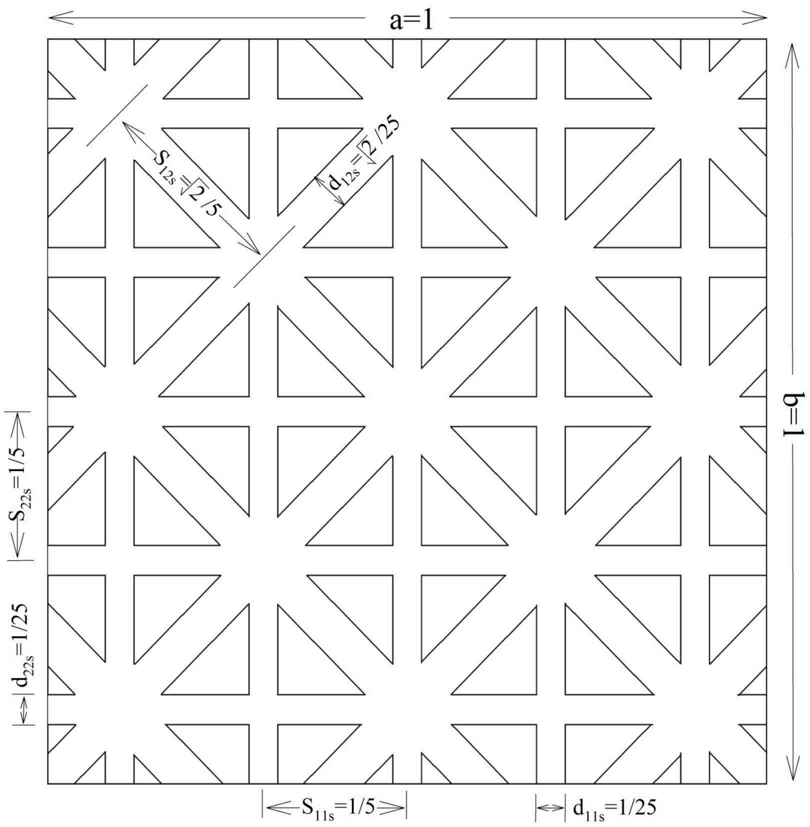


**Fig. 6.** Schematic view of the stiffener.

In order to investigate the effects of different parameters on the equilibrium paths of the stiffened piezoelectric-composite plate on the nonlinear elastic foundation, the material properties of each part need to be determined. The structural steel is selected for stiffener. The elastic modulus of stringers and rings is $E = 200GPa$. The material properties of composite plies and piezoelectric actuators are introduced in third example of the verification study. Moreover, the dimensionless parameters of the nonlinear elastic foundation are shown in forth example. The geometric parameters for the stiffeners are shown in Fig. 6.

Figures 7 and 8 show the postbuckling behavior of foundationless plates under mechanical and thermal loading, respectively. Four types of lay-up configurations are considered i.e. the symmetric cross-ply laminated composite plate [0/90], the piezolaminated plate [P/0/90], the stiffened composite plate [0/90/Stiff/90/0], and the stiffened piezo-composite plate [P/0/90/Stiff/90/0/P]. Total thickness in all of them is the same and equals to 0.01. As seen in Fig. 7, when the plate is subjected to mechanical loads, using stiffener instead of laminated composite has a lower influence on the equilibrium path especially on the buckling phenomenon. However, in Fig. 8, the thermal postbuckling behaviors improve by using concentric stiffener and surface mounted piezoelectric actuators. This is right because when the temperature is raised, the thermal stresses in stiffeners are zero.

Figures. 9 and 10 depict the postbuckling responses of sandwich composite plates with different concentric stiffeners subjected to the uniaxial compression and the uniform temperature rise, respectively. The thicknesses of composite part ($2h_c$) and stiffener ($h_s$) are 0.006 and 0.004, respectively. As can be seen in Figs. 9 and 10, the postbuckling behaviors of ortho grid stiffener is lower than angle grid and a converse trend happens in high values of dimensionless deflection. Furthermore, it is clear that there aren't any differences in case of isogrid1 and isogrid2 because of equal longitudinal and transversal half waves ($m = n = 1$). In addition, the postbuckling curves of orthotropic grid for both thermal and mechanical loadings are enhanced due to high stiffness components of the grid.

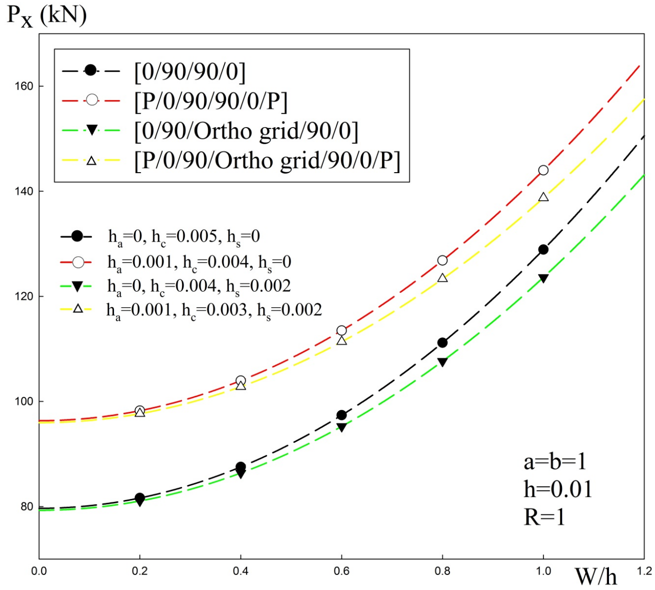


**Fig. 7.** Effects of stiffener and piezoelectric on mechanical postbuckling behaviors.

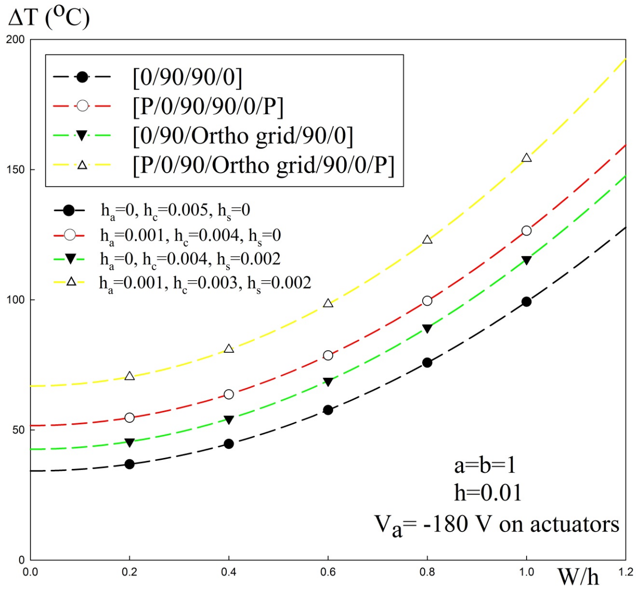


**Fig. 8.** Effects of stiffener and piezoelectric on thermal postbuckling behaviors.

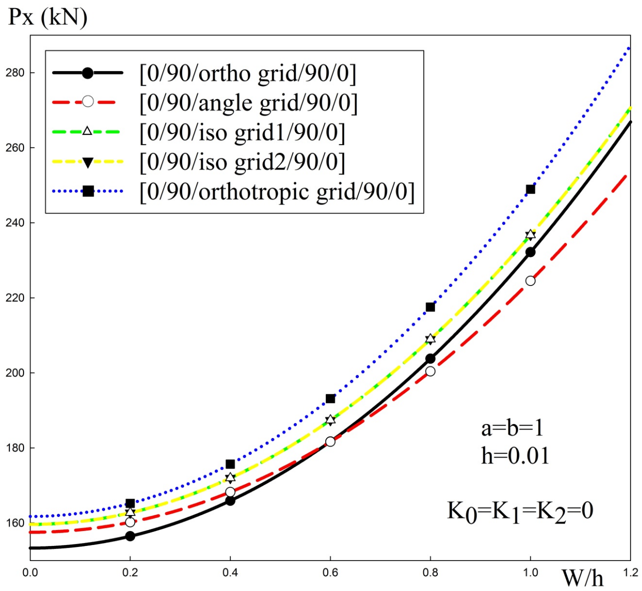


**Fig. 9.** Effects of grid shapes of concentric stiffener on mechanical postbuckling curves.

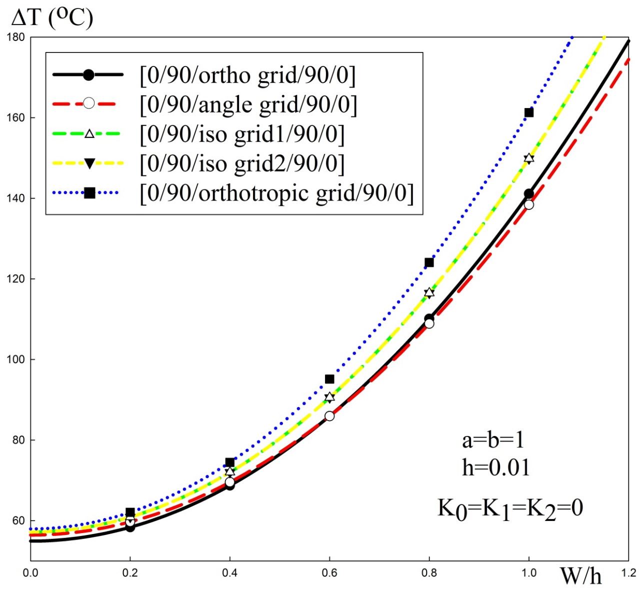


**Fig. 10.** Effects of grid shapes of concentric stiffener on thermal postbuckling curves.

Figures 11 and 12 demonstrate the effect of three parameters of foundation on the postbuckling of stiffened piezoelectric-composite plates under the biaxial compression and uniform temperature rise, respectively. The shapes of grid in concentric stiffeners are orthotropic grid and also the lay-up configuration is [P/0/90/Stiff/90/0/P]. In Fig. 11, the dimensionless Winkler and Pasternak parameters are constant and equal to 50 and 5, respectively and the nonlinear parameter changes from positive to negative quantity which means hardening to softening nonlinearity. In Fig 12, the plate rests on different types of Pasternak and the nonlinear elastic foundation and the Winkler parameter is constant. It is observed in Figs. 11 and 12 that the variations of third parameter of the elastic foundation do not affect the critical load. However, the Pasternak parameter makes the plate have a large critical load. The other important results may be extracted through these figures. The mechanical postbuckling behaviors of the plates on the softening elastic foundation ($K_2 < 0$) may experience unstable situations, while the thermal postbuckling curves of plates on the softening elastic foundation converge to neutral situations with the decrease of $K_2$.

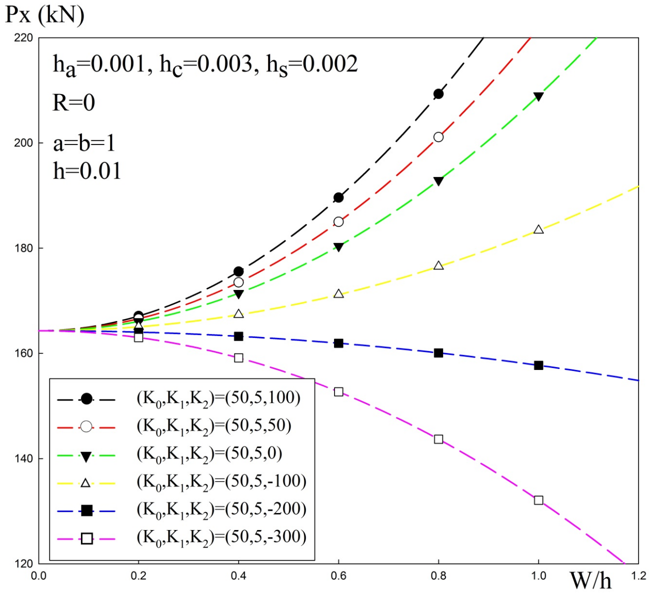


**Fig. 11.** Mechanical postbuckling behavior of stiffened piezo-composite plate on softening and/or hardening elastic foundation.

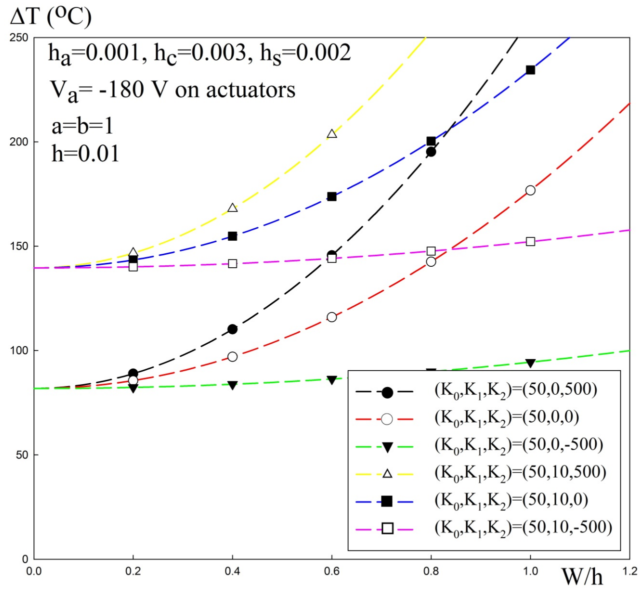


**Fig. 12.** Thermal postbuckling curves of stiffened piezoelectric-composite plate rests on different elastic foundation.

## 7. Conclusions

In the present study, a fully analytical approach was conducted to investigate the equilibrium paths of the laminated composite plate with piezoelectric actuators and different shapes of stiffeners on nonlinear elastic foundations. The plate is subjected to in-plane compressions and thermal environments. The main findings and conclusions were summarized as follows:

It was shown that the thermal postbuckling of composites with concentric stiffeners and surface mounted piezoelectric films are significantly greater than those of fully composite plates. In addition, they indicated interesting effects of different grid shapes on postbuckling paths. Moreover, it is worth noting that the hardening elastic foundation showed a good reaction on the equilibrium path. However, the softening elastic foundation may make the plate to be unstable for some loads.

## Conflict of Interest

The authors declare no conflict of interest.

## References

[1] G. Li, J. Cheng, A generalized analytical modeling of grid stiffened composite structures, *J. Compos. Mater.* 41(24) (2007) 2939-2969.
[2] H.-J. Chen, S.W. Tsai, Analysis and optimum design of composite grid structures, *J. Compos. Mater.* 30(4) (1996) 503-534.
[3] E. Wodesenbet, S. Kidane, S.-S. Pang, Optimization for buckling loads of grid stiffened composite panels, *Compos. Struct.* 60(2) (2003) 159-169.
[4] M. Hemmatnezhad, G. Rahimi, R. Ansari, On the free vibrations of grid-stiffened composite cylindrical shells, *Acta Mech.* 225(2) (2014) 609-623.
[5] M. Hemmatnezhad, G. Rahimi, M. Tajik, F. Pellicano, Experimental, numerical and analytical investigation of free vibrational behavior of GFRP-stiffened composite cylindrical shells, *Compos. Struct.* 120 (2015) 509-518.
[6] A. Talezadehlari, G. Rahimi, Comment on “Optimization for buckling loads of grid stiffened composite panels”, *Compos. Struct.* 135 (2016) 409-410.
[7] N.D. Duc, P.H. Cong, V.D. Quang, Thermal stability of eccentrically stiffened FGM plate on elastic foundation based on Reddy's third-order shear deformation plate theory, *J. Therm. Stresses* 39(7) (2016) 772-794.
[8] P.H. Cong, N. An, P. Thi, N.D. Duc, Nonlinear stability of shear deformable eccentrically stiffened functionally graded plates on elastic foundations with temperature-dependent properties, *SECM* 24(3) (2017) 455-469.
[9] S. Zhu, J. Yan, Y. Wang, M. Tong, Buckling and Postbuckling Experiments of Integrally Stiffened Panel Under Compression–Shear Loads, *J. Aircraft* 52(2) (2014) 680-691.
[10] S. Zhu, J. Yan, Z. Chen, M. Tong, Y. Wang, Effect of the stiffener stiffness on the buckling and post-buckling behavior of stiffened composite panels–Experimental investigation, *Compos. Struct.* 120 (2015) 334-345.
[11] X. Wang, W. Cao, C. Deng, P. Wang, Z. Yue, Experimental and numerical analysis for the post-buckling behavior of stiffened composite panels with impact damage, *Compos. Struct.* 133 (2015) 840-846.
[12] A.d.P.G. Villani, M.V. Donadon, M.A. Arbelo, P. Rizzi, C.V. Montestruque, F. Bussamra, M.R. Rodrigues, The

postbuckling behaviour of adhesively bonded stiffened panels subjected to in-plane shear loading, *Aerosp. Sci. Technol.* 46 (2015) 30-41.
[13] L. Huang, A.H. Sheikh, C.-T. Ng, M.C. Griffith, An efficient finite element model for buckling analysis of grid stiffened laminated composite plates, *Compos. Struct.* 122 (2015) 41-50.
[14] W. Zhao, R.K. Kapania, Buckling analysis of unitized curvilinearly stiffened composite panels, *Compos. Struct.* 135 (2016) 365-382.
[15] Y. SudhirSastry, P.R. Budarapu, N. Madhavi, Y. Krishna, Buckling analysis of thin wall stiffened composite panels, *Comp. Mater. Sci.* 96 (2015) 459-471.
[16] D. Wang, M.M. Abdalla, Global and local buckling analysis of grid-stiffened composite panels, *Compos. Struct.* 119 (2015) 767-776.
[17] R. Vescovini, C. Bisagni, Semi-analytical buckling analysis of omega stiffened panels under multi-axial loads, *Compos. Struct.* 120 (2015) 285-299.
[18] K. Nie, Y. Liu, Y. Dai, Closed-form solution for the postbuckling behavior of long unsymmetrical rotationally-restrained laminated composite plates under inplane shear, *Compos. Struct.* 122 (2015) 31-40.
[19] M. Bohlooly, B. Mirzavand, Closed form solutions for buckling and postbuckling analysis of imperfect laminated composite plates with piezoelectric actuators, *Compos. Part B: Eng.* 72 (2015) 21-29.
[20] K.M. Fard, M. Bohlooly, Postbuckling of piezolaminated cylindrical shells with eccentrically/concentrically stiffeners surrounded by nonlinear elastic foundations, *Compos. Struct.* 171 (2017) 360-369.
[21] J. Seidi, S. Khalili, K. Malekzadeh, Temperature-dependent buckling analysis of sandwich truncated conical shells with FG facesheets, *Compos. Struct.* 131 (2015) 682-691.
[22] J.N. Reddy, *Mechanics of laminated composite plates and shells: theory and analysis*, CRC press, 2004.
[23] H.-S. Shen, Post-buckling of internal-pressure-loaded laminated cylindrical shells surrounded by an elastic medium, *J. Strain Anal. Eng.* 44(6) (2009) 439-458.
[24] B. Mirzavand, M. Bohlooly, Thermal Buckling of Piezolaminated Plates Subjected to Different Loading Conditions, *J. Therm. Stresses* 38(10) (2015) 1138-1162.
[25] M.S. Boroujerdy, M.R. Eslami, Thermal buckling of piezoelectric functionally graded material deep spherical shells, *J. Strain Anal. Eng.* (2013) 0309324713484905.
[26] K. Malekzadeh, M. Khalili, R. Mittal, Local and global damped vibrations of plates with a viscoelastic soft flexible core: an improved high-order approach, *J. Sandw. Struct. Mater.* 7(5) (2005) 431-456.
[27] K. Asemi, M. Salehi, M. Akhlaghi, Three-dimensional natural frequency analysis of anisotropic functionally graded annular sector plates resting on elastic foundations, *SECM* 22(6) (2015) 693-708.
[28] H.-S. Shen, Q. Li, Postbuckling of shear deformable laminated plates resting on a tensionless elastic foundation subjected to mechanical or thermal loading, *Int. J. Solids Struct.* 41(16) (2004) 4769-4785.
[29] H.-S. Shen, Postbuckling of shear deformable laminated plates under biaxial compression and lateral pressure and resting on elastic foundations, *Int. J. Mech. Sci.* 42(6) (2000) 1171-1195.
[30] Y. Sun, S.-R. Li, R.C. Batra, Thermal buckling and post-buckling of FGM Timoshenko beams on nonlinear elastic foundation, *J. Therm. Stresses* 39(1) (2016) 11-26.
[31] H. Van Tung, N.D. Duc, Nonlinear analysis of stability for functionally graded plates under mechanical and thermal loads, *Compos. Struct.* 92(5) (2010) 1184-1191.
[32] H.-S. Shen, Thermal postbuckling of shear-deformable laminated plates with piezoelectric actuators, *Compos. Sci. Technol.* 61(13) (2001) 1931-1943.
[33] D.-G. Zhang, H.-M. Zhou, Mechanical and thermal post-buckling analysis of FGM rectangular plates with various supported boundaries resting on nonlinear elastic foundations, *Thin-Walled Struct.* 89 (2015) 142-151.

## Appendix A

Quantities of $I_i^s$, $I_i^a$, $A_{ij}$, $B_{ij}$, $D_{ij}$, and electrical and thermal resultants.

$$I_1^s = h_s, \qquad I_3^s = \frac{h_s^3}{12}$$

$$I_1^a = 2h_a, \qquad I_3^a = \frac{2}{3}\left(\frac{h_s}{2}+h_c+h_a\right)^3 - \frac{1}{3}\left(\frac{h_s}{2}+h_c\right)^3$$

$$A_{ij}, B_{ij}, D_{ij} = \sum_{k=1}^{N} \begin{Bmatrix} \bar{Q}_{11} & \bar{Q}_{12} & 0 \\ \bar{Q}_{12} & \bar{Q}_{22} & 0 \\ 0 & 0 & \bar{Q}_{66} \end{Bmatrix}_k \{(z_k - z_{k-1}), \frac{1}{2}(z_k^{\,2} - z_{k-1}^{\,2}), \frac{1}{3}(z_k^{\,3} - z_{k-1}^{\,3})\}$$

$$i, j = 1, 2, 6, \qquad -\frac{h_s}{2} - h_c < z_k < -\frac{h_s}{2} \;\;\&\;\; \frac{h_s}{2} < z_k < \frac{h_s}{2} + h_c$$

$$\begin{Bmatrix} N_x^{\ E} \\ N_y^{\ E} \\ N_{xy}^{\ E} \end{Bmatrix} = \begin{bmatrix} Q_{11}^{\ a} & Q_{12}^{\ a} & 0 \\ Q_{12}^{\ a} & Q_{22}^{\ a} & 0 \\ 0 & 0 & Q_{66}^{\ a} \end{bmatrix} \begin{Bmatrix} d_{31} \\ d_{32} \\ 0 \end{Bmatrix} \frac{V_a}{h_a} I_1^{\ a}$$

$$\begin{Bmatrix} N_x^{\ T} & M_x^{\ T} \\ N_y^{\ T} & M_y^{\ T} \\ N_{xy}^{\ T} & M_{xy}^{\ T} \end{Bmatrix} = +\sum_{k=1}^{N} \int_{z_{k-1}}^{z_k} \begin{bmatrix} \bar{Q}_{11} & \bar{Q}_{12} & 0 \\ \bar{Q}_{12} & \bar{Q}_{22} & 0 \\ 0 & 0 & \bar{Q}_{66} \end{bmatrix}_k \begin{Bmatrix} \alpha_x \Theta \\ \alpha_y \Theta \\ \alpha_{xy} \Theta \end{Bmatrix}_k (1, z)dz,$$

$$- \int_{-\frac{h_s}{2}-h_c-h_a}^{-\frac{h_s}{2}-h_c} \begin{bmatrix} Q_{11}^{\ a} & Q_{12}^{\ a} & 0 \\ Q_{12}^{\ a} & Q_{22}^{\ a} & 0 \\ 0 & 0 & Q_{66}^{\ a} \end{bmatrix} \begin{Bmatrix} \alpha_x^{\ a} \Theta \\ \alpha_y^{\ a} \Theta \\ \alpha_{xy}^{\ a} \Theta \end{Bmatrix} (1, z)dz - \int_{+\frac{h_s}{2}+h_c}^{+\frac{h_s}{2}+h_c+h_a} \begin{bmatrix} Q_{11}^{\ a} & Q_{12}^{\ a} & 0 \\ Q_{12}^{\ a} & Q_{22}^{\ a} & 0 \\ 0 & 0 & Q_{66}^{\ a} \end{bmatrix} \begin{Bmatrix} \alpha_x^{\ a} \Theta \\ \alpha_y^{\ a} \Theta \\ \alpha_{xy}^{\ a} \Theta \end{Bmatrix} (1, z)dz$$

$$-\frac{h_s}{2} - h_c < z_k < -\frac{h_s}{2} \quad \& \quad \frac{h_s}{2} < z_k < \frac{h_s}{2} + h_c$$

## Appendix B

Coefficients of $AQ_x^{\ T}$ and $AQ_y^{\ T}$.

$$\begin{Bmatrix} AQ_x^{\ T} \\ AQ_y^{\ T} \end{Bmatrix} = \begin{Bmatrix} Q_{11}^{\ a} & Q_{12}^{\ a} & 0 \\ Q_{12}^{\ a} & Q_{22}^{\ a} & 0 \end{Bmatrix} \begin{Bmatrix} \alpha_x^{\ a} \\ \alpha_y^{\ a} \\ \alpha_{xy}^{\ a} \end{Bmatrix} I_1^{\ a} + \sum_{k=1}^{N} \begin{Bmatrix} \bar{Q}_{11} & \bar{Q}_{12} & \bar{Q}_{16} \\ \bar{Q}_{12} & \bar{Q}_{22} & \bar{Q}_{26} \end{Bmatrix}_k \begin{Bmatrix} \alpha_x \\ \alpha_y \\ \alpha_{xy} \end{Bmatrix}_k (z_k - z_{k-1})$$

$$-\frac{h_s}{2} - h_c < z_k < -\frac{h_s}{2} \quad \& \quad \frac{h_s}{2} < z_k < \frac{h_s}{2} + h_c$$